MOLECULAR IMAGING AND BIOLOGY

Mol Imaging Biol (2019) 21:175–182
DOI: 10.1007/s11307-018-1216-9

Published Online: 4 June 2018

RESEARCH ARTICLE

Relationship Between Clinicopathological Characteristics and PET/CT Uptake in Esophageal Squamous Cell Carcinoma: [^{18}F]Alfatide *versus* [^{18}F]FDG

Yinjun Dong,[1,2,3] Yuchun Wei,[3,4] Guanxuan Chen,[3,5] Yong Huang,[3,6] Pingping Song,[2,3] Shuguang Liu,[2,3] Jinsong Zheng,[3,6] Monica Cheng,[7] Shuanghu Yuan[3,4,8]

[1]*Shandong University, Jinan, China*
[2]*Department of Thoracic Surgery, Shandong Cancer Hospital Affiliated to Shandong University, Jinan, China*
[3]*Shandong Academy of Medical Sciences, Jinan, China*
[4]*Department of Radiation Oncology, Shandong Cancer Hospital Affiliated to Shandong University, Jinan, China*
[5]*Department of Intensive Care Unit, Shandong Cancer Hospital Affiliated to Shandong University, Jinan, China*
[6]*Department of Nuclear Medicine, Shandong Cancer Hospital Affiliated to Shandong University, Jinan, China*
[7]*Indiana University School of Medicine (IUSM), Indianapolis, USA*
[8]*Department of Radiation Oncology, Shandong Cancer Hospital and Institute, 440 Jiyan Road, Jinan, 250117, China*

Abstract

Purpose: To assess a novel radiotracer aluminum [^{18}F]fluoride-1,4,7-triazacyclononane-triacetic acid-pegylated dimeric RGD ([^{18}F]ALF-NOTA-PRGD$_2$, denoted as [^{18}F]Alfatide) for positron emission tomography (PET)/X-ray computed tomography (CT) and explore the relationships between clinicopathological characteristics and maximum standard uptake values in primary (SUV_P) and metastatic lymph nodes (SUV_{LN}) of patients with esophageal squamous cell carcinoma (ESCC), as verified by pathologic examination and compared with those obtained with 2-deoxy-2-[^{18}F]fluoro-D-glucose ([^{18}F]DG) PET.

Procedures: We prospectively enrolled patients with newly diagnosed ESCC who agreed to undergo [^{18}F]Alfatide PET/CT or [^{18}F]FDG PET/CT scans before surgery at Shandong Cancer Hospital from May 2011 to July 2017. SUVs and the pathological tumor-node-metastasis (pTNM) stages of primary tumors and metastatic lymph nodes (LNs) were measured and confirmed pathologically. Immunohistochemical (IHC) staining for integrin αvβ3 was performed on tumor samples (both primary tumors and metastatic LNs) collected from nine patients.

Results: Of 61 patients who underwent PET/CT scans, 46 then underwent curative surgery and were included in our analysis ($n = 21$ for [^{18}F]Alfatide PET/CT and $n = 25$ for [^{18}F]FDG PET/CT). No significant differences in the SUV_P on [^{18}F]Alfatide PET/CT or [^{18}F]FDG PET/CT were observed among the cohorts according to gender, pathological stage, T stage, status of LNs, and differentiation (all $P > 0.05$). The SUV_{LN} differed significantly between the pathological stages and status of LNs both on [^{18}F]Alfatide PET/CT ($P = 0.03$, 0.003) and [^{18}F]FDG PET/CT ($P = 0.001$. < 0.001), but not according to gender ($P = 0.128$, 0.129), T stage ($P = 0.791$, 0.727), or tumor differentiation ($P = 0.049$, 0.053). Significant positive correlations were observed

Yinjun Dong and Yuchun Wei contributed equally to this work.

Correspondence to: Shuanghu Yuan; *e-mail:* yuanshuanghu@sina.com

between the SUV_{LN} on [^{18}F]Alfatide PET/CT and [^{18}F]FDG PET/CT, and pathological stage (r = 0.52, P = 0.016; r = 0.503, P = 0.01), LN status (r = 0.73, P < 0.001; r = 0.649, P < 0.001), and differentiation (r = 0.509, P < 0.019; r = 0.459, P = 0.021) were observed. No significant differences were found between the relationships of SUV_P with SUV_{LN}, length, age, gender, pathological stage, T stage, status of LN, or differentiation, or of SUV_{LN} with length, age, gender, or T stage both on [^{18}F]Alfatide PET/CT and [^{18}F]FDG PET/CT (all P > 0.05). The quantitated expression levels of αvβ3 in primary tumors and metastatic LNs were 1.67 ± 1.12 and 3.42 ± 2.93, respectively (P = 0.031).

Conclusions: Our results suggest that SUV_{LN} is influenced by pathological stage, LN status, and differentiation. SUV_{LN} may therefore serve as a new parameter for risk stratification of with ESCC patients. Moreover, [^{18}F]Alfatide PET can provide complementary molecular information about ESCC metastasis.

Key words: ^{18}F-Alfatide, [^{18}F]FDG, PET/CT, Esophageal squamous cell carcinoma, Lymph node

Introduction

2-Deoxy-2-[^{18}F]fluoro-D-glucose ([^{18}F]FDG) is the most widely used tracer for staging tumors with positron emission tomography (PET)/X-ray computed tomography (CT), a combined non-invasive metabolic imaging technique [1]. [^{18}F]FDG, as a glucose analog, enters cells through the same membrane transporters as glucose and is phosphorylated by the enzyme hexokinase. However, [^{18}F]FDG-6-phosphate is not further metabolized in the glycolytic pathway and instead is trapped in the cells in proportion to their glycolytic activity [1, 2]. Previous studies have shown that [^{18}F]FDG PET can improve preoperative staging of esophageal cancer with a sensitivity of 67–74 % and specifically benefit for the detection of non-regional lymphoid and hematologic disease [3, 4]. Although [^{18}F]FDG PET has an important role in tumor diagnosis and staging, [^{18}F]FDG is not a tumor-specific tracer, and there are false-positive results [5, 6]. For example, inflammatory cells, including macrophages and neutrophils, have a high uptake of [^{18}F]FDG, which can be shown as false positive [7, 8].

Tumor angiogenesis plays an important role in regulating its growth, local invasiveness, and metastatic potential [9]. Arginine-glycine-aspartic acid peptide (Arg-Gly-Asp, RGD) was used to detect angiogenesis by non-invasive PET imaging, which was specially combined with αvβ3, a highly expressed integrin in angiogenic tumors. A new tracer for PET has been developed using a novel one-step lyophilized kit for $PRGD_2$ peptide labeling to synthesize, aluminum [^{18}F]fluoride-1,4,7-triazacyclononane-triacetic acid-pegylated dimeric RGD ([^{18}F]ALF-NOTA-$PRGD_2$, denoted as [^{18}F]Alfatide), which has been proven to be safe [10] and able to identify non-small cell lung cancer (NSCLC) [11, 12] and glioma [13] with clarity and desirable image contrast. Previously, we performed a pilot clinical study that demonstrated the feasibility of using [^{18}F]Alfatide PET/CT to distinguish malignant lesions from hamartoma for the diagnosis of NSCLC [11]. However, use of the tracer [^{18}F]Alfatide in PET for esophageal squamous cell cancer (ESCC) staging has not been investigated.

In the present clinical study, we investigated the feasibility of [^{18}F]Alfatide PET/CT in ESCC patients and explored the relationships between clinicopathological characteristics and maximum standard uptake values in primary tumors (SUV_P) and metastatic lymph nodes (SUV_{LN}) as verified by pathologic examination and in comparison with those obtained on [^{18}F]FDG PET/CT.

Materials and Methods

Patients

Between May 2011 and July 2017, 61 patients in our hospital who were initially diagnosed with ESCC were candidates for the study. The patients underwent standard preoperative staging procedures, including physical examination, laboratory examinations, cervical and abdomen ultrasound, chest radiography, and esophagography, and recorded their clinical history. Patients who had previously been treated for cancer were excluded, as were patients with diabetes or inflammatory lung disease, as well as those who were not ineligible for surgery for medical reasons. In our institution, all patients did not metastasize to distant organs or definite directly invading adjacent organs on imaging arrangements for regular esophagectomy and extensive regional LN anatomy. We did not consider stage M1a cancer (*i.e.*, upper esophageal cancer metastasis to cervical LNs or lower esophageal cancer metastasis to celiac LNs) as contraindication for surgery. Patients with surgical diseases who refused surgery were not eligible for the study. Of the 61 patients underwent PET/CT scans, 46 underwent curative surgery as well as [^{18}F]Alfatide PET/CT (n = 21) or [^{18}F]FDG PET/CT (n = 25). PET images were taken from the cricoid to the epigastrium. All patients had a Karnofsky performance status of ≥ 80. Patients with pulmonary and/or cardiac diseases were considered ineligible for resection.

This study was approved by the ethics committee of Shandong Cancer Hospital, and each patient provided written informed consent prior to the study.

Radiotracer Preparation

A lyophilized kit for instant labeling with PRGD2 peptide and [^{18}F]FDG was purchased from the Jiangsu Institute of Nuclear Medicine, and the synthesis process was carried out as described previously [14]. The radiochemical purities of [^{18}F]FDG and [^{18}F]Alfatide exceeded 95 %, and the specific radioactivity of each exceeded 37 GBq (1000 mCi)/μmol.

PET/CT Scanning

PET/CT scans were obtained with an advanced PET/CT scanner (GEMINI TF Big Bore; Philips Healthcare). The peak voltage of the spiral CT component is 140 kV and 80 Ma, the pitch is 2:1, the slice thickness is 4.25 mm, and the rotation speed is 0.8 s per rotation. The axial range of the full-ring dedicated PET scan is the same. During image acquisition, the patient continued to perform normal shallow breathing. Image attenuation correction was performed by CT data transmission. The attenuation-corrected PET images, CT images, and fused PET/CT images were coronal, sagittal, and transaxial slices and were displayed on a MEDEX workstation (Philips Healthcare). Patients were given an intravenous injection of 4.81 MBq/kg (0.12 mCi/kg) [^{18}F]FDG or [^{18}F]Alfatide and rest for about 60 min.

Before [^{18}F]FDG PET/CT scanning, the patients fasted for at least 6 h, and each patient's blood glucose level was measured before injection of the tracer. For [^{18}F]Alfatide PET/CT scanning, fasting was not required.

No patients underwent urinary bladder catheterization or received oral muscle relaxants or CT contrast agents.

Two experienced nuclear medicine physicians read all of the images through consensus reading. PET data were reconstructed using the ordered-subsets expectation maximization algorithm. The SUVs were calculated according to the following formula: [measured activity concentration (Bq/ml) × body weight (g)]/injected activity (Bq). In the static emission scans, circular regions of interest (ROIs) with a diameter of 1.5 cm were placed over the primary tumor and metastatic LNs with the assistance of corresponding CT images. Then, the shape of the ROI circle was modulated based on the varied sizes and shapes of the malignant areas on the MEDEX workstation, and the areas with maximum intensity were chosen for measurements. Presumed LNs were reviewed after the operation.

Pathologic Evaluation of Resected Specimens

All of the patients underwent curative surgery within 3 days (mean, 1.5 days) after PET/CT scanning. A strict protocol was developed for pathologic examinations. Once the surgical specimen was available, it was oriented as closely as possible to the *in vivo* geometry, bisected in the transverse plane in the operating room by the surgeon and the pathologist, and fixed in 10 % formalin (≥ 24 h). The lengths of the tumor samples before fixation were documented by digital photography with a ruler. The palpable LNs were removed and evaluated. The total number of removed LNs and the total number of positive LNs, including their location, were recorded. Larger LNs were bisected and routine hematoxylin and eosin staining was performed according to a standardized protocol.

Immunohistochemical Staining

The excised tumor samples of nine patients were fixed in 10 % formalin and embedded in paraffin. For immunohistochemical (IHC) investigation, each tumor sample was sectioned (3- to 5-μm-thick) with a macrotome (Microm HM 450; GMI, Ramsey, MN) and stained using a biotinylated monoclonal anti-αvβ3 antibody (1:200; ab179475, Abcam). The relative expression level of αvβ3 was detected using an IHC kit (pv-6000 two-step, Zhongshan Golden Bridge Biotechnology Corporation, Beijing, China).

As mentioned earlier [15], the intensity of αvβ3-positive cells was evaluated by light microscopy. The calculated score was similar to the modified histochemical score. The positive rate of staining was divided into four grades: 0 (unstaining), 1 (weak), 2 (moderate), and 3 was strong stained. We estimate the percentage of cells stained at the different intensity levels. The total score was calculated as 0 × negative% + 1 × weak% + 2 × moderate% + 3 × strongly stained%. Then, the total staining intensity was divided into four grades: 0 (score 0–10 %), I (score 11–100 %), II (score 101–200 %), and III (score 201–300 %) [15].

Statistical Analysis

Comparisons of individual parameters, including SUVs and length, between different groups were performed with independent sample Mann-Whitney *U* tests or Kruskal-Wallis H (K) tests. The Pearson's rank correlation was used to analyze associations between SUVs and age, or length. Logistic regression analysis was used to analyze associations between SUVs and other parameters, including differentiation, stage, and gender. Statistical software (SPSS, version 17.0; SPSS Inc.) was used for all analyses. A two-sided *P* value less than 0.05 was considered significant.

Results

Patient Characteristics and Safety

The pathological tumor-node-metastasis (pTNM) stage was determined mainly by postoperative pathological data

according to the American Joint Committee on Cancer (AJCC) staging system of 2010. Images of the major organs and regions of uptake of [^{18}F]Alfatide and [^{18}F]FDG in two ESCC patients are presented in Fig. 1. The clinicopathological data of 46 ESCC patients and the differences between the groups that were summarized by [^{18}F]Alfatide PET/CT or [^{18}F]FDG PET/CT are summarized in Table 1. Of these patients, 4 had stage I disease, 17 had stage II, 24 had stage III, and 1 had stage IV. Also, 7 had T1 ESCC, 10 had T2, 22 had T3, and 4 had T4. No statistical differences in age ($P = 0.868$), length ($P = 0.139$), gender ($P = 0.31$), differentiation ($P = 0.492$), pathological stage ($P = 0.351$), T stage ($P = 0.286$), and status of LNs ($P = 0.689$) between the two groups.

No adverse or clinically detectable pharmacologic effects related to PET/CT with either tracer were detected in any of the patients. In addition, no significant changes in vital signs or the results of laboratory studies or electrocardiography were observed.

Difference in SUVs

The differences in SUVs according to the different characteristics of ESCC patients are summarized in Table 2. No significant differences in SUV_P on [^{18}F]Alfatide PET/CT were observed with differing gender ($P = 0.40$), pathological stage ($P = 0.374$), T stage ($P = 0.205$), status of LNs ($P = 0.744$), or differentiation ($P = 0.484$), and the results were consistent for SUVp on [^{18}F]FDG PET/CT ($P = 0.575$, 0.81, 0.134, 0.511, and 0.71, respectively). A significant difference was observed in the SUV_{LN} with differing pathological stage and LN status of LN on [^{18}F]Alfatide PET/CT ($P = 0.03$ and 0.001, respectively) and on [^{18}F]FDG PET/CT ($P = 0.002$ and < 0.001, respectively), but not with differences in gender ($P = 0.128$ and 0.129, respectively), T stage ($P = 0.791$ and 0.727, respectively), or tumor differentiation ($P = 0.049$ and 0.053, respectively).

Correlations between SUVs and Clinicopathological Characteristics

The correlations between the SUVs and clinical parameters are listed in Table 3. Significant positive correlations were observed between the SUV_{LN} on both [^{18}F]Alfatide PET/CT and [^{18}F]FDG PET/CT and the pathological stage ($r = 0.52$, $P = 0.016$ and $r = 0.503$, $P = 0.01$, respectively), LN status ($r = 0.73$, $P < 0.001$ and $r = 0.649$, $P < 0.001$, respectively), and tumor differentiation ($r = 0.509$, $P < 0.019$ and $r = 0.459$, $P = 0.021$, respectively). The relationships between SUV_P and SUV_{LN}, length, age, gender, pathological stage, T stage, LN status, and differentiation as well as between SUV_{LN} and length, age, gender, and T stage showed no statistical differences both on [^{18}F]Alfatide PET/CT and [^{18}F]FDG PET/CT (all $P > 0.05$).

Immunohistochemistry Validations

Samples from 9 of 46 patients were randomly selected for validation of the integrin αvβ3 expression patterns by IHC examination on 9 primary tumor specimens and 6 metastatic LNs. Two representative images of stained sections are shown in Fig. 2. On all pathological sections, staining for integrin αvβ3 was limited to ESCC tumor cells and observed mainly in the cytoplasm of these cells. The quantitated expression levels of αvβ3 in primary tumors and metastatic LNs were 1.56 ± 0.73 and 1.0 ± 0.02, respectively ($P = 0.068$).

Discussion

With the advancement of image analysis tools and three-dimensional display techniques, tumor metabolic characteristics can now be assessed rapidly and consistently with no interobserver variability, and could potentially be applied routinely in clinical practice. Studies on the capabilities of RGD PET/CT have increased in recent years, and showed the potential advantages of this imaging technique for evaluating brain and chest tumors due to the high tumor-to-background ratio *in vivo* on PET imaging. Chen et al. found that the primary lung boundary effects of RGD PET imaging are similar to those of [^{18}F]FDG PET, and RGD PET provides better imaging of mediastinal LNs and contralateral lung metastases [16]. In the present clinical study, [^{18}F]Alfatide PET/CT showed the same efficacy as [^{18}F]FDG PET/CT based on assessment of the differences in SUVs and correlations between SUVs and clinicopathological characteristics in ESCC patients. Thus, our results indicate that [^{18}F]Alfatide PET can provide complementary molecular information about ESCC metastasis.

Tumor stage is used to describe the degree of disease and tumor invasiveness. It is an important parameter to guide treatment decision and evaluate prognosis. It has been showed that [^{18}F]FDG PET/CT is a valuable tool for the primary staging of esophageal carcinoma [17]. SUVmax can reflect the degree of tumor invasion and nodal invasion [17]. Several studies have investigated the relationship between the [^{18}F]FDG PET/CT SUVmax and tumor stage, and a significant association was found between SUVmax and the stage of esophageal cancer, with increased SUV uptake correlating with advanced tumor stage [17, 18]. Therefore, we also explored the relationships between tumor state and SUV_P or SUV_{LN} on [^{18}F]Alfatide and [^{18}F]FDG PET/CT. In this study, SUV_{LN} on both [^{18}F]Alfatide and [^{18}F]FDG PET/CT was positively correlated with the pathological stage and LN status. However, our results did not indicate a significant difference in the SUV_P with differing pathological stage, T stage, or status of LN status for ESCC both on either [^{18}F]Alfatide or [^{18}F]FDG PET/CT. Moreover, our results did not demonstrate any associated trends, which may most likely be due to the selection bias of patients.

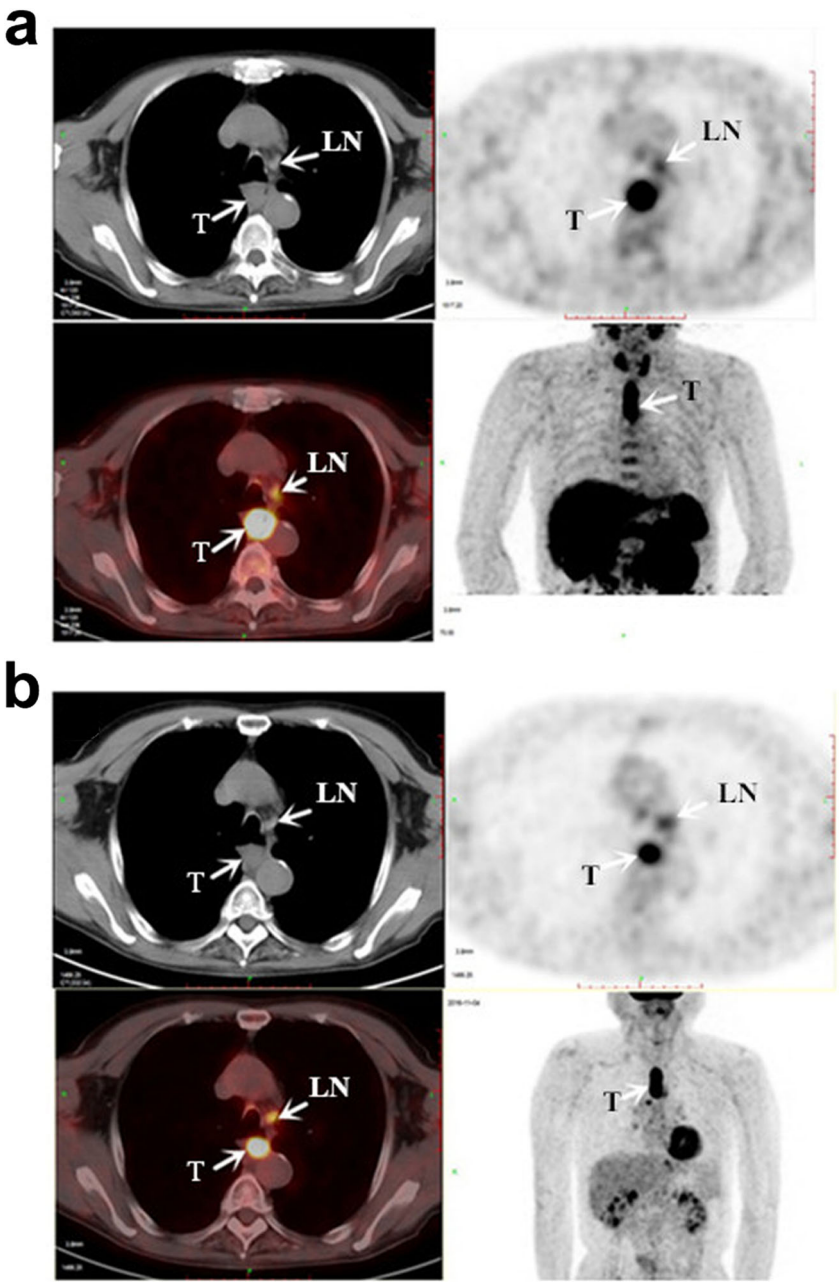

Fig. 1 PET/CT images of major organs and regions of uptake at 1 h after injection of **a** [^{18}F]Alfatide or **b** [^{18}F]FDG PET/CT in the same patient with upper-middle esophageal squamous cell carcinoma (ESCC). T, primary tumor; LN, metastatic lymph node.

Previous studies have shown that SUVmax of the primary tumor is useful for determining prognosis in patients with esophageal carcinoma [19, 20]. Studies before showed that the SUVmax is associated with the differentiation of lung cancer as well as head and neck cancer [19, 21]. However, previous studies on esophageal cancer have been limited, with inconsistent results [22, 23]. Therefore, this study investigated the relationships between the SUV_P or SUV_{LN} and tumor differentiation of ESCC. It was found that there was a positive correlation between the degree of differentiation of ESCC primary lesions and SUVmax [22]. However, Mu et al. [23] found that SUVmax was not significantly correlated with the differentiation for a heterogeneous group of esophageal cancer tumors. It is well-known that tumors often drive inflammation both in primary tumor tissue and tumor-draining LNs. The inflamed tissue can also show high uptake of [^{18}F]FDG and [^{18}F]Alfatide [24]. In this study, the uptake measurements for primary tumors and LNs on [^{18}F]FDG and [^{18}F]Alfatide PET were based on the result of enhanced CT and verified by postoperative pathological examination to reduce the risk of false-positive results. For the analyzed group of ESCC patients, only the SUV_{LN}, and

Table 1. . Clinicopathological data of 46 esophageal squamous cell carcinoma patients and the difference between the two groups

	[^{18}F]Alfatide PET/CT patients (*n*)	[^{18}F]FDG PET/CT patients (*n*)	*P*
Total	21	25	
Age, years (median)	62(47–81)	61(47–79)	0.868
Length, cm (median)	5.0 (2–10)	5.0 (1–12)	0.139
Sex (%)			0.31
Female	7(33.3)	5(20.0)	
Male	14(66.7)	20(80.0)	
Differentiation (%)			0.492
Well	7(33.3)	5(20.0)	
Moderate	5(23.8)	8(32.0)	
Poor	9(42.9)	12(48.0)	
Pathological stage			0.351
I–II	8(38.1)	13(52.0)	
III–IV	13(61.9)	12(48.0)	
T stage			0.286
T1–T2	6(28.6)	11(44.0)	
T3–T4	15(71.4)	14(56.0)	
Status of LN (%)			0.689
N−	8(38.1)	11(44.0)	
N+	13(61.9)	14(56.0)	

LN, lymph node; *N*−, negative LN; *N*+, positive LN

not SUV_P, was positively correlated with tumor differentiation for both, [^{18}F]Alfatide and [^{18}F]FDG PET/CT. This discrepancy may be partly attributed to patient selection, as a previous study demonstrated that squamous cell carcinoma may exhibit different PET/CT uptake than adenocarcinoma.

Immunohistochemical staining confirmed the expression of integrin αvβ3 predominantly on ESCC cells. Notably, the IHC staining intensity observed in this study was lower than that in a previous study [15] that evaluated αvβ3 expression on head and neck cancer, glioblastoma, and breast cancer tumor cells as well as tumor microvessels, and also found αvβ3 expression only on melanoma tumor cells. In the present study, no integrin αvβ3 expression was found on the ESCC tumor vasculature. Currently, αvβ3 is assumed to have both positive and negative regulatory roles in angiogenesis, depending on the respective biological context [25]. Due to the low number of samples in our study and the small size of the specimens, an exact analysis of αvβ3 expression was not feasible. Consequently, no exact correlation between αvβ3 expression on IHC and [^{18}F]Alfatide uptake could be determined, which is a limitation of our study. Prior research [26] indicated that primary tumor length is a prognostic factor for overall survival (OS) in ESCC patients [27, 28] and tumor length, as measured by [^{18}F]FDG PET/CT or

Table 2. . Difference in SUVs of the different characteristics in patients with ESCC

	SUV_P		SUV_{LN}	
	[^{18}F]Alfatide PET/CT	[^{18}F]FDG PET/CT	[^{18}F]Alfatide PET/CT	[^{18}F]FDG PET/CT
Sex (%)				
Female	6.08 ± 1.64	16.40 ± 11.34	2.59 ± 1.0	3.57 ± 0.69
Male	5.59 ± 1.91	14.46 ± 5.21	3.25 ± 0.89	6.07 ± 3.47
P	0.4	0.575	0.128	0.129
Pathological stage				
I–II	6.35 ± 2.06	14.99 ± 8.16	2.41 ± 1.06	4.02 ± 1.83
III–IV	5.39 ± 1.60	14.69 ± 4.73	3.41 ± 0.68	7.24 ± 3.70
P	0.374	0.81	0.03	0.002
T stage				
T1–T2	6.39 ± 1.67	12.40 ± 7.96	3.10 ± 1.07	5.17 ± 2.23
T3–T4	5.50 ± 1.84	16.77 ± 4.76	3.0 ± 0.95	5.88 ± 3.95
P	0.205	0.134	0.791	0.727
Status of LN				
N+	5.55 ± 1.67	13.97 ± 6.01	3.57 ± 0.58	7.41 ± 3.35
N−	6.09 ± 2.07	15.97 ± 7.42	2.16 ± 0.80	3.23 ± 0.44
P	0.744	0.511	0.001	< 0.001
Differentiation				
Well	5.71 ± 2.42	15.89 ± 6.08	2.44 ± 0.83	3.26 ± 0.36
Moderate	6.36 ± 2.03	16.22 ± 7.54	2.91 ± 0.62	4.49 ± 1.67
Poor	5.45 ± 1.15	13.49 ± 6.44	3.56 ± 0.98	7.05 ± 4.02
P	0.484	0.71	0.049	0.053

SUV_P, standard uptake value of primary tumor; SUV_{LN}, standard uptake value of metastatic lymph node

Table 3. . Correlation between SUVs and clinicopathological characteristics with [^{18}F]Alfatide PET/CT and [^{18}F]FDG PET/CT in patients with ESCC

	[^{18}F]Alfatide PET/CT		[^{18}F]FDG PET/CT	
	r	P	r	P
SUV_P and SUV_{LN}	0.069	0.766	0.18	0.39
SUV_P and length	0.175	0.448	0.374	0.066
SUV_P and age	0.09	0.699	0.093	0.659
SUV_P and pathological stage	0.265	0.245	0.023	0.913
SUV_P and T stage	0.23	0.316	0.336	0.101
SUV_P and status of LN	0.15	0.515	0.154	0.463
SUV_P and differentiation	0.05	0.828	0.152	0.467
SUV_{LN} and length	0.114	0.624	0.212	0.309
SUV_{LN} and age	0.093	0.687	0.325	0.112
SUV_{LN} and sex	0.333	0.141	0.313	0.128
SUV_{LN} and pathological stage	0.52	0.016	0.503	0.01
SUV_{LN} and T stage	0.009	0.843	0.11	0.601
SUV_{LN} and status of LN	0.73	< 0.001	0.649	< 0.001
SUV_{LN} and differentiation	0.509	0.019	0.459	0.021

SUV_P, SUV of primary tumor; *LN*, lymph node; *SUV_{LN}*, SUV of metastatic LN

PET, is associated with the stage and OS of esophageal cancer [29]. Feng et al. [22] demonstrated that the SUV_P was positively correlated with tumor length. However, our current findings showed that primary tumor length, as measured by pathology, did not correlate with any of the measured SUVs in ESCC. The esophagus is a flexible, moving muscular organ; therefore, a single largest tumor diameter on PET/CT or other conventional imaging does not represent the real tumor size or tumor burden because the tumor does not always have a uniform shape or a homogeneous composition. Moreover, the methods for determining the boundaries of primary tumors differed between the studies, and the optimal threshold of SUV for tumor delineation needs to be further explored. Another possibility is that tumor volume or weight would be more accurate for correlation analyses with PET imaging parameters rather than tumor length, and further research is needed to confirm this idea.

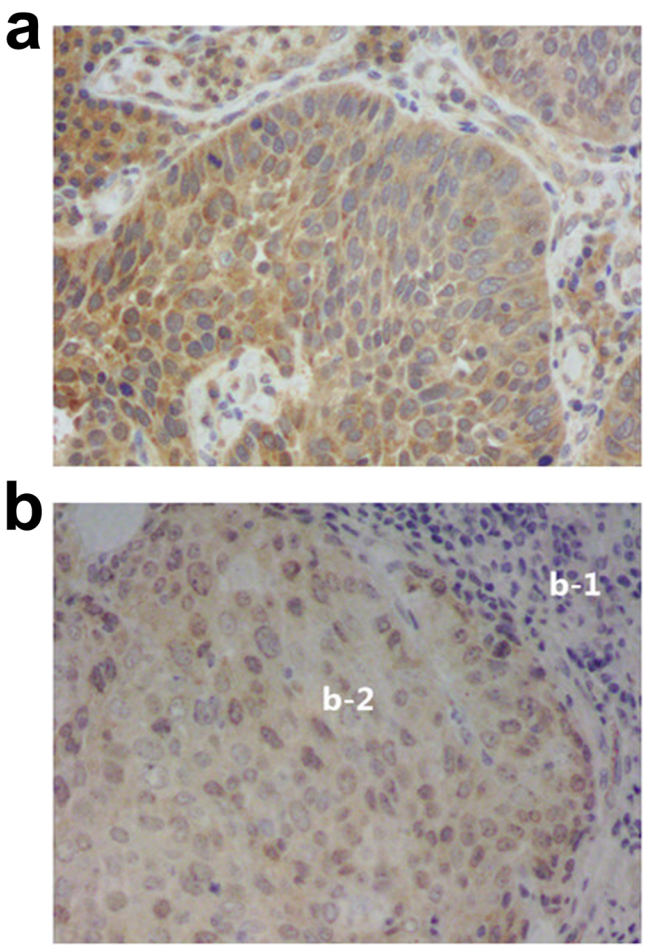

Fig. 2 Patterns of IHC staining for integrin αvβ3 in resected samples. **a** Moderate αvβ3 staining of primary ESCC tumor (200×). **b** Weak staining for αvβ3 staining in metastatic LN (B-1) *versus* no staining in normal LN tissue (B-2; 200×).

LN involvement is a well-characterized negative factor affecting survival in patients with esophageal cancer; the cure rate in patients with affected nodes is significantly lower than that in patients without. The accurate assessment of locoregional LNs in esophageal cancer is the key for not only staging purposes but also the application of precision medicine. Our current findings on the SUV_{LN}-based parameter of PET/CT suggest new ways to stratify patients with ESCC, as SUV_{LN} better reflected of the clinical features of ESCC than did SUV_P.

Our study is inherently limited by its confinement to a single center and a limited number of patients. We did not analyze differences in SUVs of according to age and tumor length because these criteria have no clear grouping criteria. An additional study is required to recruit a larger sample size of ESCC patients to explore the criteria or cutoff value for age and tumor length.

Conclusion

The differences in SUVs and correlations between SUVs on [^{18}F]Alfatide or [^{18}F]FDG PET/CT and the

clinicopathological characteristics of ESCC were consistent between the imaging approaches. Our present findings on the SUV_{LN}-based parameter of PET/CT suggest new ways to stratify patients with ESCC and that [^{18}F]Alfatide PET can provide complementary molecular information about ESCC metastasis.

Acknowledgments. The authors extend their gratitude to Professor Yongsheng Gao (Department of Pathology, Shandong Cancer Hospital and Institute) for his help with IHC analysis and Jianbo Zhang (Department of Pathology, Shandong Cancer Hospital and Institute) for his help with the IHC examination.

Funding. This study was partially funded by the Special Fund for Scientific Research in the Public Interest (201402011), the National Key Research and Development Plan (2016YFC0904700), the Natural Science Foundation of China (NSFC81172133, NSFC81372413), the Shandong Key Research and Development Plan (2017CXGC1209 and 2017GSF18164), and the Outstanding Youth Natural Science Foundation of Shandong Province (JQ201423).

Compliance with Ethical Standards. This study was approved by the ethics committee of Shandong Cancer Hospital, and each patient provided written informed consent prior to the study.

Conflict of Interest

The authors declare that they have no conflict of interest.

References

1. Czernin J, Phelps ME (2002) Positron emission tomography scanning: current and future applications. Annu Rev Med 53:89–112
2. Phay JE, Hussain HB, Moley JF (2000) Strategy for identification of novel glucose transporter family members by using internet-based genomic databases. Surgery 128:946–951
3. Flamen P, Lerut A, Van Cutsem E et al (2000) Utility of positron emission tomography for the staging of patients with potentially operable esophageal carcinoma. J Clin Oncol 18:3202–3210
4. Heeren PA, Jager PL, Bongaerts F, van Dullemen H, Sluiter W, Plukker JT (2004) Detection of distant metastases in esophageal cancer with ^{18}F-FDG PET. J Nucl Med 45:980–987
5. Strauss LG (1996) Fluorine-18 deoxyglucose and false-positive results: a major problem in the diagnostics of oncological patients. Eur J Nucl Med 23:1409–1415
6. van Westreenen HL, Heeren PA, Jager PL et al (2003) Pitfalls of positive findings in staging esophageal cancer with F-18-fluorodeoxyglucose positron emission tomography. Ann Surg Oncol 10:1100–1105
7. Ishimori T, Saga T, Mamede M, Kobayashi H, Higashi T, Nakamoto Y, Sato N, Konishi J (2002) Increased (18)F-FDG uptake in a model of inflammation: concanavalin A-mediated lymphocyte activation. J Nucl Med 43:658–663
8. Kubota R, Yamada S, Kubota K, Ishiwata K, Tamahashi N, Ido T (1992) Intratumoral distribution of fluorine-18-fluorodeoxyglucose in vivo: high accumulation in macrophages and granulation tissues studied by microautoradiography. J Nucl Med 33:1972–1980
9. Hood JD, Cheresh DA (2002) Role of integrins in cell invasion and migration. Nat Rev Cancer 2:91–100
10. Wu C, Yue X, Lang L, Kiesewetter DO, Li F, Zhu Z, Niu G, Chen X (2014) Longitudinal PET imaging of muscular inflammation using ^{18}F-DPA-714 and ^{18}F-Alfatide II and differentiation with tumors. Theranostics 4:546–555
11. Gao S, Wu H, Li W, Zhao S, Teng X, Lu H, Hu X, Wang S, Yu J, Yuan S (2015) A pilot study imaging integrin αvβ3 with RGD PET/CT in suspected lung cancer patients. Eur J Nucl Med Mol Imaging 42:2029–2037
12. Luan X, Huang Y, Gao S, Sun X, Wang S, Ma L, Teng X, Lu H, Yu J, Yuan S (2016) ^{18} F-alfatide PET/CT may predict short-term outcome of concurrent chemoradiotherapy in patients with advanced non-small cell lung cancer. Eur J Nucl Med Mol Imaging 43:2336–2342
13. Zhang H, Liu N, Gao S, Hu X, Zhao W, Tao R, Chen Z, Zheng J, Sun X, Xu L, Li W, Yu J, Yuan S (2016) Can an ^{18}F-ALF-NOTA-PRGD2 PET/CT scan predict treatment sensitivity to concurrent chemoradiotherapy in patients with newly diagnosed glioblastoma. J Nucl Med 57:524–529
14. Wan W, Guo N, Pan D, Yu C, Weng Y, Luo S, Ding H, Xu Y, Wang L, Lang L, Xie Q, Yang M, Chen X (2013) First experience of ^{18}F-alfatide in lung cancer patients using a new lyophilized kit for rapid radiofluorination. J Nucl Med 54:691–698
15. Beer AJ, Haubner R, Sarbia M, Goebel M, Luderschmidt S, Grosu AL, Schnell O, Niemeyer M, Kessler H, Wester HJ, Weber WA, Schwaiger M (2006) Positron emission tomography using [^{18}F]Galacto-RGD identifies the level of integrin alpha(v)beta3 expression in man. Clin Cancer Res 12:3942–3949
16. Chen X, Sievers E, Hou Y, Park R, Tohme M, Bart R, Bremner R, Bading JR, Conti PS (2005) Integrin alpha v beta 3-targeted imaging of lung cancer. Neoplasia 7:271–279
17. Thurau K, Palmes D, Franzius C, Minin E, Senninger N, Juergens KU, Bruewer M (2011) Impact of PET-CT on primary staging and response control on multimodal treatment of esophageal cancer. World J Surg 35:608–616
18. Suzuki A, Xiao L, Hayashi Y, Macapinlac HA, Welsh J, Lin SH, Lee JH, Bhutani MS, Maru DM, Hofstetter WL, Swisher SG, Ajani JA (2011) Prognostic significance of baseline positron emission tomography and importance of clinical complete response in patients with esophageal or gastroesophageal junction cancer treated with definitive chemoradiotherapy. Cancer 117:4823–4833
19. Cerfolio RJ, Bryant AS (2006) Maximum standardized uptake values on positron emission tomography of esophageal cancer predicts stage, tumor biology, and survival. Ann Thorac Surg 82:391–394; discussion 394-395
20. Rizk N, Downey RJ, Akhurst T, Gonen M, Bains MS, Larson S, Rusch V (2006) Preoperative ^{18}F-fluorodeoxyglucose positron emission tomography standardized uptake values predict survival after esophageal adenocarcinoma resection. Ann Thorac Surg 81:1076–1081
21. Vesselle H, Schmidt RA, Pugsley JM, Li M, Kohlmyer SG, Vallires E, Wood DE (2000) Lung cancer proliferation correlates with [F-18]fluorodeoxyglucose uptake by positron emission tomography. Clin Cancer Res 6:3837–3844
22. Feng R, Li MH, Kong L, Shi F, Yang GR, Yu JM (2009) Correlation between PET-CT ^{18}FDG uptake in primary lesions and clinicopathological parameters in esophageal carcinoma patients. Zhonghua Zhong Liu Za Zhi 31:452–454
23. Mu DB, Wang SP, Yang WF et al (2007) Correlation between FDG PET/CT and the expression of glutl and ki-67 antigen in esophageal cancer. Zhonghua Zhong Liu Za Zhi 29:30–33
24. Wu C, Yue X, Lang L, Kiesewetter DO, Li F, Zhu Z, Niu G, Chen X (2014) Longitudinal PET imaging of muscular inflammation using ^{18}F-DPA-714 and 18F-Alfatide II and differentiation with tumors. Theranostics 4:546–555
25. Hynes RO (2002) A reevaluation of integrins as regulators of angiogenesis. Nat Med 8:918–921
26. Sun M, Li B, Fu Z et al (2013) Relationship between 18F-fluorodeoxyglucose uptake in primary lesions and clinicopathological characteristics of esophageal squamous cell carcinoma patients. Exp Ther Med 5:170–174
27. Liu H, Lu L, Zhu Q, Hao YT, Mo YX, Liu M, Hu YH, Cui NJ, Rong TH (2011) Cervical nodal metastases of unresectable thoracic esophageal squamous cell carcinoma: characteristics of long-term survivors after concurrent chemoradiotherapy. Radiother Oncol 99:181–186
28. Eloubeidi MA, Desmond R, Arguedas MR, Reed CE, Wilcox CM (2002) Prognostic factors for the survival of patients with esophageal carcinoma in the U.S.: the importance of tumor length and lymph node status. Cancer 95:1434–1443
29. Roedl JB, Sahani DV, Colen RR, Fischman AJ, Mueller PR, Blake MA (2008) Tumour length measured on PET-CT predicts the most appropriate stage-dependent therapeutic approach in oesophageal cancer. Eur Radiol 18:2833–2840